INFLUENCE OF PRECIPITATES AND THEIR DISTRIBUTION ON SEAWATER CORROSION RESISTANCE OF Al-Mg ALLOY①

Lin Leyun, Zhang Qihai, Yang Zhimin
Beijing General Research Institute for Nonferrous Metals, Beijing 100088

ABSTRACT The corrosion behaviors of Al-Mg alloy LF6M plates(5xxx series) exposed to seawater are significantly different. These alloy plates with different precipitate distribution states had been full-immersed in Qingdao, Xiamen and Yulin sea areas for 1, 2, 4 and 8 a respectively, and then were heat-treated and probed by SEM and TEM before they were put into the seawater again. The experimental results showed that the intergranular corrosion morphology occurring on the corrosion specimens are well-related to the states and sorts of the precipitates and the inclusions located at the grain boundaries, especially chain-distributed $(MnFe)Al_6$ and silicates produced by special heat-treatment. The electrochemical measurement of the specimens also gave reasonable explanations for the difference of their corrosion behaviors.

Key words Al-Mg alloy seawater corrosion resistance precipitate

1 INTRODUCTION

LF6M Al-Mg alloy (5xxx series with Mg content 6%) has been widely used in marine engineering because of its higher strength and excellent corrosion resistance. It is well known that the β phase (the intermetallic compound with rich magnesium content) precipitated at grain boundaries can deteriorate the corrosion resistance of Al-Mg alloys with higher magnesium content[1-3]. The existence of Mn as alloy content and Fe as impurity can lead to $(MnFe)Al_6$ precipitates[2, 4] in the alloys and seems to influence the corrosion resistance of the alloys[3, 5]. Unfortunately, the phenomenon and the mechanism are seldom reported. Since 1982, 11 types of Al alloys have been exposed to marine environment at China National Test Network to get seawater corrosion data of 1, 2, 4, 8, 16 a intervals, including the LF6M alloy made in China. After 1, 2, 4 a intervals the alloy (with Al clad) exibited good resistance to seawater corrosion, but severe local corrosion occurred on one specimen exposed for 8 a, where the Al clad was consumed thoroughly[6]. The initial study shows that it is the $(MnFe)Al_6$ precipitate at grain boundaries of the alloy that is responsible for the severe local corrosion[7].

The present work will further study the influence of $(MnFe)Al_6$ precipitate on the seawater corrosion behavior of the alloy and the specimens will be heat-treated again so as to control the microstructure of the alloy in correspondence with the corrosion behavior of the alloy exposed to seawater for 1 a.

2 EXPERIMENTAL

2.1 Experimental materials and apparatus

The experiment materials are annealing plates of 5 mm thick from manufactory, the composition of which is shown in Table 1. The size of the specimens is 100 mm × 200 mm. The Al clad layers of the specimens were removed by alkaline washing before they were heat-treated again in vacuum furnace. The treatment technologies are represented by A, B and C, the heat treatment temperatures of which are 550, 320, and 450 ℃, respectively[8, 9].

① Supported by the National Natural Science Foundation of China Received Mar. 29, 1996; accepted Jul. 22, 1996

Table 1 Composition analysis of LF6M alloy

Components	Mg	Mn	Ti	Al
Content/%	6.4	0.64	0.096	Rem.
Components	Fe	Si	Cu	Zn
Content/%	0.21	0.12	< 0.1	< 0.15

The experimental apparatus used are JSM 840 SEM fitted with TN 5500 EDX, JEM 2000FX TEM fitted with LINKAN 1000 EDX, 1250 potentiostat from Solartran Co., and microcomputer of Macintosh with corresponding soft ware.

2.2 Experimental methods

Three types of standard specimens were full-immersed in Xiamen seawater for one year according to the method provided by China national standard GB6384-86, the microstructures of which were observed by transmission electron microscopy (TEM), scanning electron microscopy (SEM) and optical microscopy (OM). Specimens for TEM observation are thin films prepared by electrolytic double spray technique, and specimens for OM observation are cross sections of the original specimens or those after seawater corrosion test, both of which are specimens for SEM. The specimens for electrochemical measurement are small plates of 10 mm × 10 mm cut from the standard specimens with welded electrode wire and polished surface.

3 RESULTS AND DISCUSSION

3.1 Microstructure observation

Three types of microstructures were observed by SEM and TEM, corresponding to three types of heat-treatment technologies A, B and C. As shown in Fig. 1 (SEM picture of thin film specimen), microstructure of chain-like precipitates along grain boundaries is taken from the specimen corresponding to heat-treatment technology A. The microstructure can be divided into three levels, that is, dark grey matrix, light grey particles a little bit higher than matrix and white particles much higher than matrix. According to semiquantitative composition analysis, the light grey particles can be represented by $(MnFe)Al_{6.4}$, approximately equal to intermetallic compound $(MnFe)Al_6$, and the white particles are phases of silicate. The particles of $(MnFe)Al_6$ or silicate are as long as 1~10 μm. The phases of $(MnFe)Al_6$ are 1 μm long with structure of orthorhombic system distributed at the grain boundaries of the matrix which possesses the face central cubic (*FCC*) structure. The structure of silicate can not be identified because it is too thick to be transmitted by electron beam. Most of them are also located at the grain boundaries. Fig. 2 shows a TEM diffraction con-

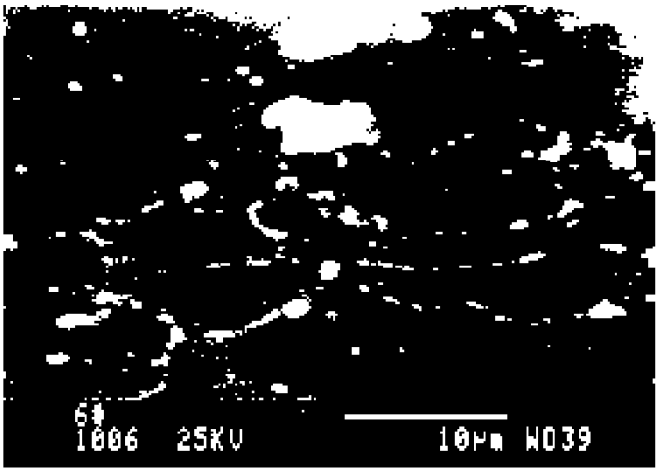

Fig. 1 SEM image of chain-like precipitates in specimens of LF6M treated by technology A

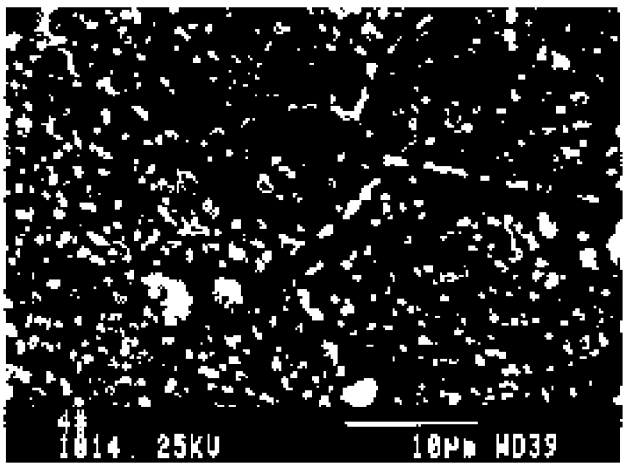

Fig. 2 TEM image of precipitates on grain boundaries, × 25 000

trast image of a grain boundary with precipitates on it using the same specimen as that of Fig. 1.

Fig. 3 shows a microstructure corresponding to the specimen of technology B, with a large amount of β phase (Mg rich phase) distributed on the matrix. No characteristic of distribution of precipitates along grain boundaries can be seen in the figure. Although the structure of specimens of technology C is similar to that of technology A, the precipitates are much less and not distributed along grain boundaries (figure omitted).

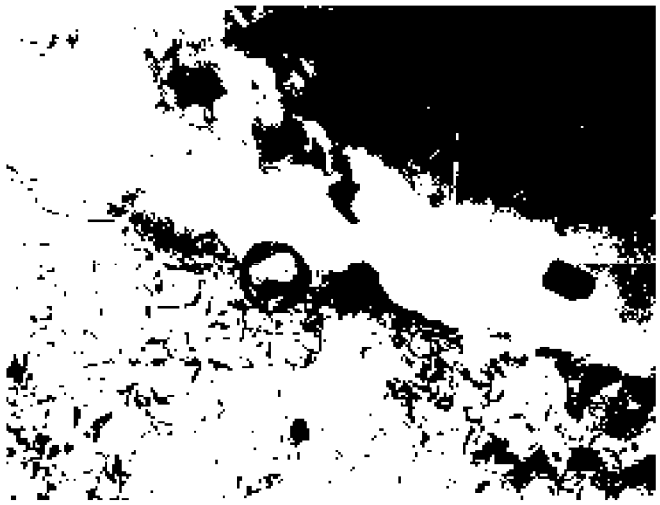

Fig. 3 SEM image of microstructure of the specimens treated by technology B
(β phase grains spread in the alloy matrix)

3.2 Analyses of corrosion specimens

After one year exposure to seawater, severe local corrosion occurred only on the specimens treated by technology A. Fig. 4 is a sketch of corrosion pit section, in which the numbers stand for the points of composition analyses by SEM and EDX, and the analysis results are given in Table 2. The morphology of the pitting is intergranular as shown in Fig. 5, which is taken from the pit bottom of the specimen by means of OM. Fig. 5 shows that corrosion developed parallel to the surface of the specimen once the pitting went deep into the matrix of the alloy. Therefore, the shape of the pit in Fig. 5 is something like a calabash with a small orifice. Because of the intergranular corrosion morphology shown in Fig. 5, the composition of every point probed includes elements of Cl, S, Ca, etc., indicating that the corrosion products were probed simultaneously. From the results of Table 2, the following conclusions can be drawn:

(1) No extremely high Mn content was detected, indicating the relatively uniform distribution of Mn.

(2) The contents of Ti (alloying element), Fe and Si (impurities) are higher in some local places, suggesting a tendency to form inclusion. The average content of Si is much higher than its name content in the alloy (see Table 1), and as high as 10.79% and 7.23% at point 1 and point 5, respectively. The contents of Fe at the two points are also higher than other points, indicating that the two impurities were richened at the two places and deteriorated the corrosion resist-

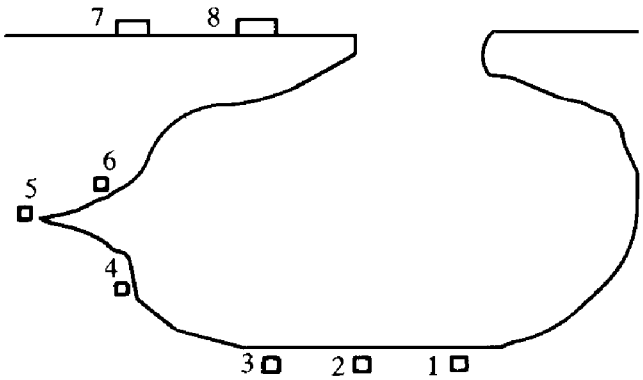

Fig. 4 The pitting sketch of specimens treated by technology A after exposed to seawater for 1 a

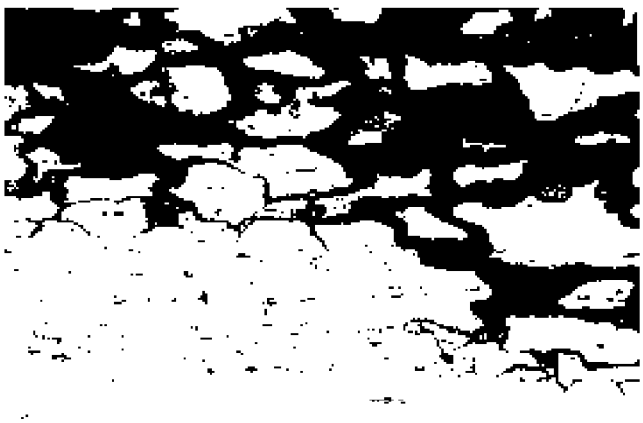

Fig. 5 The intergranular corrosion morphology of the bottom of the pitting shown in Fig. 4, × 200

Table 2 The composition analyses of different positions along the pitting edge of LF6M specimens(%)

Points	1	2	3	4	5	6	7	8
Al	79.53	91.36	91.54	91.02	70.73	90.97	90.94	91.70
Mg	5.90	6.60	6.68	6.33	8.18	6.53	7.18	6.58
Mn	0.50	0.52	0.47	0.52	0.26	0.87	0.52	0.53
Ti	0.30	0.03	0.26	0.28	7.16	0.38	0.54	0.30
Si	10.79	0.82	0.53	0.92	7.27	0.62	0.34	0.61
Fe	1.58	0.35	0.15		2.23		0.04	0.10
Cl	0.23	0.16	0.14	0.19	0.33	0.14	0.10	0.08
S	0.37	0.12	0.14	0.68	2.09	0.48	0.26	0.11
Ca	0.79	0.04	0.08	0.06	1.75	0.00	0.07	0.00

ance of these places. According to literature[5], Si and Fe as impurities in Al alloys could decrease the temperature of solid solubility of Mn in the alloys, so as to promote precipitation of $(MnFe)Al_6$. It might be the high content of the impurities that makes $(MnFe)Al_6$ precipitate at the grain boundaries as mentioned above. There should be precipitation-free zones near the precipitates at grain boundaries with corrosion potential lower than that of the precipitate and also lower than that of the alloy matrix, which act as an anode of corrosion process and make intergranular corrosion occur.

(3) At point 1 and point 5, the highest contents of Cl, S and Ca were detected, which is the indicator of severe corrosion.

3.3 Electrochemical measurement results

Fig. 6 shows the anodic polarization curves measured by potentiostatic determination conducted in 3.5% NaCl solution at room temperature. Two typical curves were obtained by measuring the specimens corresponding to technologies A and B (abbr. Tec. A and Tec. B), respectively.

The problems of Tec. A can be seen by analysis of the two curves. Although the curve of Tec. B exhibits a little bit stronger tendency of corrosion in weak polarization zone, it is noticed that a plateau arises near 10^{-3} mA current zone, indicating a wider passivation zone existing on the polarization curve. Comparatively speaking, the passivation zone of Tec. A is 40 mV narrow, that is, the specimen would enter active zone earlier as anodic polarization proceeds. It can be seen from Fig. 6 that, the anodic current of Tec. A is two orders higher than that of Tec. B when the specimens are potentiostatically polarized to − 730 mV. Obviously, the anodic polarization behavior of specimens treated by Tec. B would not change greatly if the areas of the specimens used in electrochemical measurement were limited to grain boundary zone, while for the specimens treated by Tec. A, the pitting potential would decrease and the anodic current density would increase greatly. Moreover, the corrosion potential of Al-Mg alloys exposed to seawater

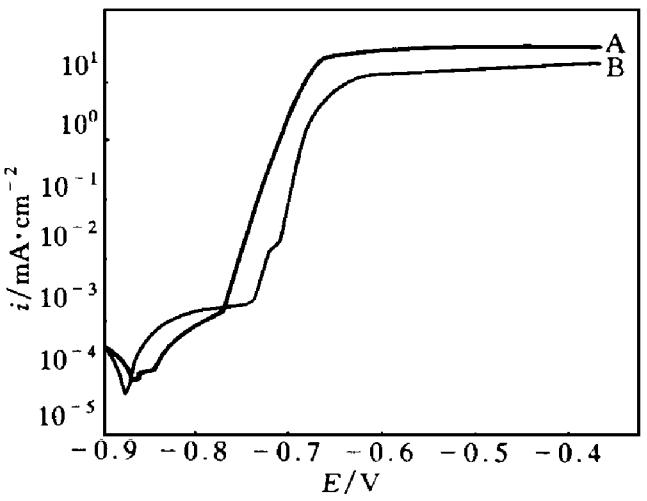

Fig. 6 Comparison of two anodic polarization curves corresponding to specimens treated by Tec. A and Tec. B

(NaCl aqueous solution 3.5%, pH 8.2, room temperature)

(To page 124)

laser pressure and the antishock pressure of vaporation; the results of the interaction between the expansion stress and the mechanical pressure show positive oscillation in the oscilloscope. In comparison with the building-up of the wave, the attenuation of the stress wave is very slow.

4 CONCLUSIONS

(1) LSP can effectively improve LY12CZ aluminum alloy's mechanical properties.

(2) With the increase of the laser power density, the material's surface hardness and fatigue strength can be improved evidently.

(3) After the LSP, there are quite a lot of dislocations forming in the materials, which is the main reason to improve the material's fatigue strength.

(4) The stress wave includes two parts: one is the heat elastic shock wave which comes from the expansion stress, the other is the mechanical pressure which arises from the laser pressure and the antishock pressure of vaporation.

REFERENCES

1 Willian F Bate Jr. Appl of Laser in Material Processing Proceeding of Conference. Washington, DC: AMS, 1979: 317- 330.
2 Fairland B P, Wilcox B A. Appl Phys, 1972, 43(9): 3893- 3895.
3 Fairland B P, Clauer A H. Appl Phys Lett, 1974, 25: 431.
4 Clauer A H, Fairland B P. Metall Trans A, 1977, 8A: 119.
5 Gao Zhentong *et al*. Fatigue Application Statistics, (in Chinese). Beijing: National Defence Press, 1986: 282- 304.
6 Hertzberg R W. Deformation and Fracture Mechanics of Engineering Materials. John Wiley & Sons, 1987.

(Edited by Peng Chaoqun)

(From page 119)

will shift to - 700~ - 750 mV[10] as pH values decrease to 7.2(due to the attachment of marine organism, for example). In that case, the specimens treated by Tec. A will suffer severe local corrosion.

4 CONCLUSION

The chain-like and network-distribution (Mn, Fe) Al_6 and silicate compound precipitated at grain boundaries in the specimens heat-treated by particular technology can severely deteriorate the corrosion resistance of LF6M Al-Mg alloy exposed to natural seawater.

REFERENCES

1 John E. Aluminium-Properties and Metallurgy. Ohio: Metals Park, ASM, 1984.
2 Chen Zuxiu. In: Proc Sec Inter Conf on Al Alloys. Beijing: 1990: 682.
3 Li Jiuqing, Tu Yidong. Cailiao Baohu, (in Chinese), 1994, 27(4): 1.
4 Zhang Baochang. Nonferrous Metals and Their Heat-treatment. Beijing: Nat Def Ind Pub, 1981: 8.
5 Zhu Zufang (ed). Corrosion Resistance of Nonferrous Metals and Their Application. Beijing: Chem Ind Pub, 1995: 6.
6 Lin Leyun, Song Wensang. In: 7th APCCC Proceedings. Beijing: 1990, 1: 541.
7 Yan Yumin, Lin Leyun, Wang Xiaohua. Corr Sci and Prot Tech, (in Chinese), 1995: 7(3): 225.
8 Czirki A *et al*. In: Proc Sec Inter Conf on Al Alloys. Beijing: 1990: 508.
9 Zheng Yuzhen *et al*. Eng Mater, (in Chinese), 1994, 8- 9: 7.
10 Rowland H T *et al*. Corrosion, 1980, 36(9): 458.

(Edited by Li Jun)